International Journal of Electrical and Computer Engineering (IJECE)
Vol. 14, No. 5, October 2024, pp. 5117~5130
ISSN: 2088-8708, DOI: 10.11591/ijece.v14i5.pp5117-5130

Optimal control design of the COVID-19 model based on Lyapunov function and genetic algorithm

Aminatus Sa'adah[1,2], Roberd Saragih[2], Dewi Handayani[2]
[1]Department of Informatics Engineering, Telkom University Purwokerto, Banyumas, Indonesia
[2]Department of Mathematics, Institut Teknologi Bandung, Bandung, Indonesia

Article Info

Article history:

Received Feb 19, 2024
Revised Jul 10, 2024
Accepted Jul 17, 2024

Keywords:

COVID-19
Genetic algorithm
Lyapunov control function
Optimal control
The SEIR model
Vaccination

ABSTRACT

Millions of people died worldwide as a result of the coronavirus disease 2019 (COVID-19) pandemic that started in early 2020. Examining the COVID-19 susceptible-exposed-infected-recovery (SEIR) mathematical model is one approach to developing the best control scenario for this disease. The study utilized two control variables, vaccination, and therapy, to construct a control function that relied on the quadratic Lyapunov function. The control objective was to lower the number of COVID-19 infections while maintaining system stability. A genetic algorithm (GA) is used as a novel method to estimate controller parameter value to replace the previously used parameter tuning procedure. Then, a numerical simulation was carried out implementing three control scenarios, namely vaccination control only, treatment control only, and vaccination and treatment control simultaneously. Based on the results, scenario 3 (vaccination and treatment simultaneously) showed the most significant decrease: the average decrease in the exposed human population was 98.29%, and the infected human population was 98.18%.

Corresponding Author:

Aminatus Sa'adah
Department of Informatics Engineering, Telkom University Purwokerto
Banyumas, 5347, Indonesia
Email: aminatus@ittelkom-pwt.ac.id

1. INTRODUCTION

World Health Organization (WHO) announced a global pandemic caused by coronavirus disease 2019 (COVID-19) in March 2020. COVID-19, caused by a novel human coronavirus, severe-acute-respiratory-syndrome-related coronavirus-2 (SARS-CoV-2), first appeared in Wuhan, China, at the end of December 2019. The disease causes several symptoms, including difficulty breathing, cough, runny nose, odynophagia, headache, fever or chills, muscle or body aches, vomiting or diarrhea, shortness of breath, and a new loss of taste or smell [1]. The primary target of this virus is the respiratory system, and COVID-19's respiratory symptoms can range widely from mild symptoms to severe hypoxia and acute respiratory distress syndrome (ARDS) [2]. Several researchers have conducted in-depth research regarding the SARS-CoV-2 virus to create effective and safe drugs and vaccines to treat this disease. It is essential to do this, considering that COVID-19 has caused millions of deaths globally [3]–[5].

Mathematical models can be an alternative to preliminary research before conducting clinical trials of vaccination and treatment scenarios for patients. In [6], a mathematical model of high-risk parasitic worm clonorchiasis was used to conduct an analytical and numerical examination of vaccine recommendations. While a vaccine to cure this condition has not yet been developed, this mathematical model is the first reference point. A mathematical model of dengue fever transmission was constructed in [7], [8] to determine the efficacy of Wolbachia release as a biological control in stopping the spread of the Aedes aegypti

mosquito, which serves as a vector for the dengue fever virus. The analysis of dynamics of the COVID-19 dissemination were described by the susceptible-exposed-infected-recovery (SEIR) model in [9]–[11]. In [11], this model separates the symptomatic and asymptomatic infected compartments into two groups.

Control variables such as treatment and vaccination have been discussed in the SEIRCOVID-19 model in several studies [12]–[16]. Applying these control variables aims to reduce the spread of COVID-19 in the population by reducing the number of infected and exposed humans. However, the control method used does not contain the uncertainty and robustness factors of the model, and the parameter values are not estimated based on real data. Model parameter values need to be estimated based on real data to obtain more precise simulation results based on real conditions in the population [17]–[19]. Different approaches have been taken to improve modeling concerning the new coronavirus using genetic algorithms. genetic algorithms (GA) were developed in the mid-1960s by Holland by using the natural selection process to inspire fresh, improved, and varied approaches to optimization challenges [20].

Lyapunov control is usually used in the field of mechanical models [21], [22]. In this research, a Lyapunov function-based control method will be constructed that can stabilize the SEIR model while achieving control objectives. Then, a new approach is used, using a genetic algorithm to estimate optimal control parameter values to replace the parameter tuning process that has been carried out so far. The model parameter values will be estimated based on actual data using a genetic algorithm. A genetic algorithm is a search algorithm that mimics the process of natural selection to find the optimal solution to a problem. In this study, the optimal solution is when the model satisfies the control objective and Lyapunov stability criteria [23], [24]. Next, the model will be analyzed for stability, and numerical simulations will be carried out based on the proposed Lyapunov control design. Three control scenarios will be carried out, namely vaccination control only, treatment control only, and vaccination and treatment control simultaneously.

This research is structured as follows: section 1 contains the introduction and formulation of the problem. Section 2 provides an explanation of the mathematical model formulation of the spread of COVID-19, analysis of the dynamics of the COVID-19 model including the model equilibrium point, the basic reproduction number, stability analysis of the equilibrium point. Section 3 presents the results, which involve the estimation of parameters for the COVID-19 model, the development of a control design using a quadratic Lyapunov function, and the numerical simulation of the control design's application and interpretation. Finally, section 4 provides a conclusion from the entire research.

2. RESEARCH METHOD

The research flow in this work consists of four main stages, namely model formulation, model dynamic analysis, controller design determination, and numerical simulation and result analysis. The main topic discussed in this research is determining optimal control in minimizing the spread of COVID-19. This research uses parameter values sourced from previous research obtained from the parameter estimation process. The brief research methodology of this work is shown in Figure 1.

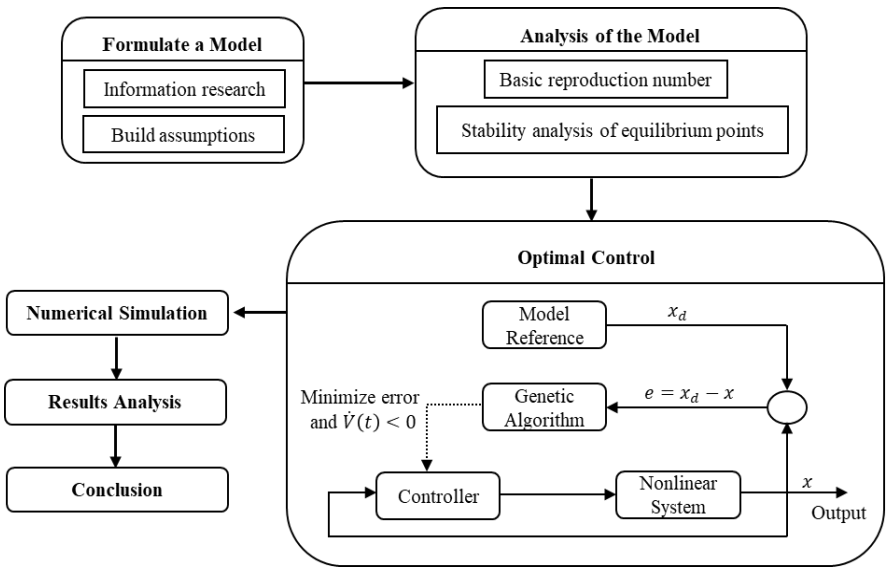

Figure 1. Research methodology

2.1. Formulate a model

In this stage, a SEIR mathematical model will be prepared that describes the dynamics of the spread of COVID-19 in a population. The model was built based on [17], [18] using several assumptions as problem constraints to facilitate model formulation. The assumptions used in this research are that the birth rate and the death rate are the same; the population is closed; there is no movement (migration, mobility) from or to the observed area; every human being is born into a susceptible population; types of death are natural, deaths from COVID-19 are ignored; and immunity is not immune, meaning that individuals who already have immunity can lose immunity and re-enter the susceptible population [11], [25].

2.2. Analysis the model

At this stage, an analysis of the model's dynamics is carried out, consisting of determining the basic reproduction number (R_0) and analyzing the stability of the model's equilibrium point. This aims to determine the important conditions of the model as knowledge in constructing controllers and implementing numerical simulations. The amount of R_0 is calculated using the next generation matrix by determining the largest absolute eigenvalue by first determining the Jacobian matrix around the non-endemic equilibrium point. Local stability analysis is determined by linearizing the model around the equilibrium point using the Jacobian matrix.

2.3. Optimal control

At this stage, optimal control is constructed based on the Lyapunov function and genetic algorithm optimization. The objective function of the controller is to achieve a stable condition and reduce the number of individuals infected with COVID-19. First, the COVID-19 model that has been prepared will be called the actual nonlinear system. Then, a reference model was formed as a tracking system that will describe ideal conditions, namely non-endemic conditions with no spread of the COVID-19 disease. Next, a controller based on the Lyapunov function is designed to estimate the control parameter values using a genetic algorithm with a fitness function that minimizes the error between the actual model output and the reference model and reaches the condition. When the error between the actual model output and the reference model reaches a minimum, the actual model has succeeded in moving along with the reference model toward non-endemic conditions.

2.4. Numerical simulation

In this stage, a numerical simulation of the control design is carried out. Three control scenarios will be reviewed to see the different effect of every control variable, namely control vaccination (u_1) only, control treatment (u_2) only, and control u_1 and u_2 simultaneously. Numerical simulations were carried out using the 4th order Runge-Kutta method. The model parameter values use reference values from previous research, while the initial values used refer to conditions at a certain time. The numerical simulation also aims to determine the effectiveness of the control design that has been prepared by calculating the percentage reduction in the number of cases with and without control.

3. RESULTS AND DISCUSSION

3.1. Results of model formulation

The proposed of a mathematical model for the spread of COVID-19 based on [10], [26] requires basic assumptions, defining compartments and parameters, and explaining disease transmission between compartments. The proposed model was divided the total population N into four subpopulations, namely susceptible (S), exposed (E), infected (I), and immune (R). In this model, the immune individuals are individuals who already have immunity to COVID-19, both natural immunity and immunity from vaccines. There are two control variables, namely vaccination (u_1) and treatment (u_2). The definition of the model parameters is presented in Table 1.

Table 1. The definition of model parameter

Parameter	Definition	Unit	Value
b	Natural birth rate	Human.Day^{-1}	$\frac{1}{70{,}69\times365}$ [26]
μ	Natural death rate	Day^{-1}	$\frac{1}{70{,}69\times365}$ [26]
β	Transmission rate	Day^{-1}	0.30379 [26]
α	The transition rate of exposed to infectious individual	Day^{-1}	0.22235 [26]
ε	Recovery rate	Day^{-1}	0.33229 [26]
ϕ	Waning immunity rate	Day^{-1}	$\frac{1}{180}$ [26]

Each compartment of the model can increase or decrease in number at any time t. Control of vaccination u_1 was given to susceptible and exposed individuals at rates of u_1pS and u_1pE, respectively. Susceptible and exposed individuals who have been vaccinated will move into immune individuals. Susceptible individuals increase because the recruitment rate bN. Unvaccinated susceptible individuals $(1-u_1p)S$ can become exposed individuals if they interact with infected individuals with a transmission rate of $(1-u_1p)\beta SI/N$. The exposed individuals move into infected individuals after passing the incubation period at a rate of α. The parameter α can be interpreted as the inverse of the length of the incubation period. Infected individuals can recover through treatment control u_2 and switch to immune individuals at a rate of $(1+u_2)\varepsilon I$. Based on the assumption that immunity is temporary, immune individuals can lose their immunity and return to susceptible individuals at a rate of ϕR. Each compartment can be reduced by natural death at a rate of μ [26]. A transmission diagram illustrating the interactions of each compartment is given in Figure 2. According to the above explanation, we obtain the mathematical model of COVID-19 with control as in system (1):

$$\begin{aligned}
\dot{S} &= b + \phi R - (1-u_1p)\beta SI - u_1pS - \mu S,\\
\dot{E} &= (1-u_1p)\beta SI - (\alpha+\mu)E - u_1pE,\\
\dot{I} &= \alpha E - (1+u_2)\varepsilon I - \mu I,\\
\dot{R} &= (1+u_2)\varepsilon I + u_1pS + u_1pE - (\phi+\mu)R,
\end{aligned} \tag{1}$$

where $S+E+I+R=1$ and initial condition $S(0), E(0), I(0), R(0) \geq 0$.

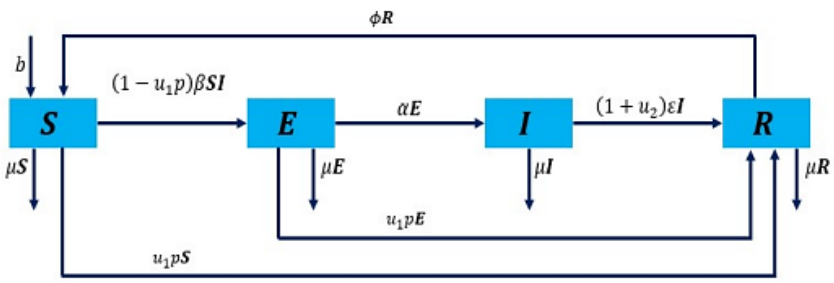

Figure 2. Transmission diagram of the COVID-19 model

3.2. Results of analysis of the model's dynamics

This section examines the dynamics of the mathematical model that describes the spread of COVID-19 in the absence of any control measures ($u_1 = u_2 = 0$). It includes an examination of the equilibrium point, basic reproduction number, and the stability analysis of the equilibrium point. The following system (2) is a mathematical model of COVID-19 without control:

$$\begin{aligned}
\dot{S} &= b + \phi R - \beta SI - u_1pS - \mu S,\\
\dot{E} &= \beta SI - (\alpha+\mu)E - u_1pE,\\
\dot{I} &= \alpha E - \varepsilon I - \mu I,\\
\dot{R} &= \varepsilon I + u_1pS + u_1pE - (\phi+\mu)R,
\end{aligned} \tag{2}$$

The equilibrium points of the model in system (2) is obtained when the rate of change of a subpopulation over time is zero, namely when $\dot{S} = \dot{E} = \dot{I} = \dot{R} = 0$ [27]. The mathematical model describes in system (2) possesses two equilibrium points, namely the disease-free equilibrium E_0 and the endemic equilibrium point E_1. The disease-free equilibrium point is a condition when there is no spread of disease in the population, namely $E = 0$ and $I = 0$ [28]. Based on the calculations, the non-endemic equilibrium point is $E_0 = (S_0, E_0, I_0, R_0) = (b/\mu, 0,0,0)$. Based on the assumption of positivity of all parameters, the equilibrium points E_0 always exists. The endemic equilibrium point is a condition where the disease spreads in the population, namely $E \neq 0$ and $I \neq 0$. The endemic equilibrium points of the system (2) is $E_1 = (S^*, E^*, I^*, R^*)$ where

$$\begin{aligned}
S^* &= (\alpha+\mu)(\varepsilon+\mu)/\alpha\beta,\\
E^* &= \big((\mu+)(\mu+\varepsilon)^2(\alpha+\mu)(R_0-1)\big)/\alpha\beta\big((\alpha+\mu)(\phi+\varepsilon+\mu)+\phi\varepsilon\big),
\end{aligned}$$

$I^* = (\alpha + \mu)(\mu + \phi)(\mu + \varepsilon)(R_0 - 1)/\beta\big((\alpha + \mu)(\phi + \varepsilon + \mu) + \phi\varepsilon\big)$, and
$R^* = \big(\varepsilon(\alpha + \mu)(\mu + \varepsilon)(R_0 - 1)\big)/\beta\big((\alpha + \mu)(\phi + \varepsilon + \mu) + \phi\varepsilon\big)$.

Therefore, the endemic equilibrium point E_1 exists if $R_0 > 1$.

3.2.1. Basic reproduction number (R_0)

The basic reproduction number R_0 is one of the important parameters in the epidemic model. In a population that is fully susceptible, the basic reproduction number indicates the number of secondary infection cases that were passed on by a single primary infection case [29]. The basic reproduction number is a threshold quantity that indicates whether an epidemic will occur or not. If the basic reproduction number (R_0) is less than 1, the infection will become extinct. Conversely, if R_0 is more than 1, an epidemic will occur. The value of R_0 will be computed using the next generation matrix (NGM) as described in reference [5]. Based on system (2) defined vector $\mathrm{x} = (E, I)^T$ then decompose x into $F - V$ form as follows:

$$F = \begin{pmatrix} \beta SI \\ 0 \end{pmatrix} \text{ and } V = \begin{pmatrix} (\alpha + \mu)E \\ -\alpha E + (\varepsilon + \mu)I \end{pmatrix},$$

where matrix F represents disease transmission and matrix V represents disease transition. Next, the NGM matrix is obtained from the formula $NGM = \mathbb{F}\mathbb{Z}^{-1}$ with $\mathbb{F} = \frac{\partial F}{\partial \mathbf{x}}\Big|_{E_0}$ and $\mathbb{Z} = \frac{\partial V}{\partial \mathbf{x}}\Big|_{E_0}$ [30]. The NGM matrix corresponding to the disease-free equilibrium point E_0 is as (3):

$$NGM = \begin{pmatrix} \frac{\beta\alpha S}{(\alpha+\mu)(\varepsilon+\mu)} & \frac{\beta S}{(\varepsilon+\mu)} \\ 0 & 0 \end{pmatrix}.$$

So that the basic reproduction number obtained from system (2) is:

$$R_0 = \frac{\alpha\beta b}{\mu(\alpha+\mu)(\mu+\varepsilon)} \tag{3}$$

Disease-free conditions will occur if the disease is not epidemic or infection has not occurred, namely when $R_0 < 1$. Note that the term b represents the parameters for the occurrence of infection in the population. Meanwhile, the term $(\alpha + \mu)(\mu + \varepsilon)$ represents the parameters related to the reduction of infection in the population. Thus, the condition that describes the disease is not endemic or infection has not occurred if the infection rate is less than the cure and death rate.

3.2.2. The stability analysis of equilibrium point

The mathematical model of COVID-19 describes in system (2) takes the form of a system of nonlinear differential equations. Therefore, the stability analysis is carried out by linearization around the equilibrium point using the Jacobian matrix [29]. The Jacobian matrix of system (2) is obtained by partially deriving the four equations f_1 to f_4 with respect to compartments S, E, I, and R, respectively, as:

$$J = \begin{pmatrix} \frac{\partial f_1}{\partial S} & \frac{\partial f_1}{\partial E} & \frac{\partial f_1}{\partial I} & \frac{\partial f_1}{\partial R} \\ \frac{\partial f_2}{\partial S} & \frac{\partial f_2}{\partial E} & \frac{\partial f_2}{\partial I} & \frac{\partial f_2}{\partial R} \\ \frac{\partial f_3}{\partial S} & \frac{\partial f_3}{\partial E} & \frac{\partial f_3}{\partial I} & \frac{\partial f_3}{\partial R} \\ \frac{\partial f_4}{\partial S} & \frac{\partial f_4}{\partial E} & \frac{\partial f_4}{\partial I} & \frac{\partial f_4}{\partial R} \end{pmatrix}$$

where
$f_1 = \dot{S} = b + \phi R - \beta SI - \mu S$
$f_2 = \dot{E} = \beta SI - (\alpha + \mu)E$
$f_3 = \dot{I} = \alpha E - (\varepsilon + \mu)I$
$f_4 = \dot{R} = \varepsilon I - (\phi + \mu)R$

We obtained the Jacobian of the system (2) is:

$$J = \begin{pmatrix} -\beta \boldsymbol{I} - \mu & 0 & -\beta \boldsymbol{S} & \phi \\ \beta \boldsymbol{I} & -(\alpha + \mu) & \beta \boldsymbol{S} & 0 \\ 0 & \alpha & -(\varepsilon + \mu) & 0 \\ 0 & 0 & \varepsilon & -(\phi + \mu) \end{pmatrix} \tag{4}$$

The stability analysis of the disease-free equilibrium (DFE) point E_0 and endemic equilibrium point E_1 of system (2) is given by the following theorems:

Theorem 1. The non-endemic equilibrium (DFE) point E_0 is asymptotically stable if $R_0 < 1$.

Proof. The Jacobian matrix (4) evaluated at the non-endemic equilibrium point E_0 of system (2) is as (5):

$$J_0 = \begin{pmatrix} -\mu & 0 & -\frac{\beta b}{\mu} & \phi \\ 0 & -(\alpha + \mu) & \frac{\beta b}{\mu} & 0 \\ 0 & \alpha & -(\varepsilon + \mu) & 0 \\ 0 & 0 & \varepsilon & -(\phi + \mu) \end{pmatrix}. \tag{5}$$

The eigen values of the Jacobian matrix J_0 are $\lambda_1 = -\mu$, $\lambda_2 = -(\mu + \phi)$, and $\lambda_{3,4}$ are the root of the equation

$$\lambda^2 + \lambda(\alpha + 2\mu + \varepsilon) + \big((\alpha + \mu)(\mu + \varepsilon)(1 - R_0)\big) = 0. \tag{6}$$

The eigen values $\lambda_{3,4}$ will be negative if $\big((\alpha + \mu)(\mu + \varepsilon)(1 - R_0)\big) > 0$, it means when $R_0 < 1$. The equilibrium point E_0 will asymptotically stable if all of the eigen values are negative. Therefore, the non-endemic equilibrium point E_0 is asymptotically stable if $R_0 < 1$.

Theorem 2. The endemic equilibrium point E_1 is asymptotically stable if $R_0 > 1$, $\left(\frac{c_1}{\alpha\beta S^*}\right) > 1$, $\left(\frac{c_2}{\alpha\beta S^*(\mu+\phi)}\right) > 1$, and $\frac{a_1 c_1 + \alpha\beta^2(\mu+\phi)}{a_1 \alpha\beta S^* + c_2} > 1$, where

$a_1 = \beta I^* + \alpha + 3\mu + \phi + \varepsilon$,
$c_1 = (\beta I^* + \mu)(\alpha + 2\mu + \phi + \varepsilon) + \alpha(\mu + \varepsilon) + \phi(\alpha + \varepsilon)$, and
$c_2 = \beta I^*[(\mu + \phi + \varepsilon)(\alpha + \mu) + \phi\varepsilon] + (\mu + \alpha)[\mu(\mu + \phi + \varepsilon) + \phi\varepsilon]$.

Proof. The Jacobian matrix (4) evaluated at the endemic equilibrium point E_1 of system (2) is as (7):

$$J_1 = \begin{pmatrix} -\beta \boldsymbol{I}^* - \mu & 0 & -\beta \boldsymbol{S}^* & \phi \\ \beta \boldsymbol{I}^* & -(\alpha + \mu) & \beta \boldsymbol{S}^* & 0 \\ 0 & \alpha & -(\varepsilon + \mu) & 0 \\ 0 & 0 & \varepsilon & -(\phi + \mu) \end{pmatrix}. \tag{7}$$

The eigen values of Jacobian matrix J_1 are $\lambda_1 = -\mu$ and $\lambda_{2,3,4}$ are the root of the qubic (8):

$$\lambda^3 + a_1\lambda^2 + a_2\lambda + a_3 = 0, \tag{8}$$

where $a_1 = \beta I^* + \alpha + 3\mu + \phi + \varepsilon$, $a_2 = c_1 - \alpha\beta S^*$, $a_3 = c_2 - \alpha\beta S^*(\mu + \phi)$, $c_1 = (\beta I^* + \mu)(\alpha + 2\mu + \phi + \varepsilon) + \alpha(\mu + \varepsilon) + \phi(\alpha + \varepsilon)$, and $c_2 = \beta I^*[(\mu + \phi + \varepsilon)(\alpha + \mu) + \phi\varepsilon] + (\mu + \alpha)[\mu(\mu + \phi + \varepsilon) + \phi\varepsilon]$.

Based on Routh-Hurwitz criteria, the roots of (8) will have negative real part if a_1,a_2,$a_3 > 0$ and $a_1 a_2 - a_3 > 0$. Therefore, we obtained as follows:

- Because of all the parameter is positive and $I^* \geq 0$, then $a_1 > 0$.
- The coefficient $a_2 > 0$ if $\left(\frac{c_1}{\alpha\beta \boldsymbol{S}^*}\right) > 1$.
- The coefficient $a_3 > 0$ if $\left(\frac{c_2}{\alpha\beta \boldsymbol{S}^*(\mu+\phi)}\right) > 1$.
- The term $a_1 a_2 - a_3 > 0$ will satisfied if $\frac{a_1 c_1 + \alpha\beta^2(\mu+\phi)}{a_1 \alpha\beta \boldsymbol{S}^* + c_2} > 1$.

The endemic equilibrium point E_1 will be asymptotically stable if all of the eigenvalues are negative. Hence, the endemic equilibrium point E_1 will be asymptotically stable if $R_0 > 1$, $\left(\frac{c_1}{\alpha\beta S^*}\right) > 1$, $\left(\frac{c_2}{\alpha\beta \boldsymbol{S}^*(\mu+\phi)}\right) > 1$, and $\frac{a_1 c_1 + \alpha\beta^2(\mu+\phi)}{a_1 \alpha\beta \boldsymbol{S}^* + c_2} > 1$.

3.3. Results of optimal control construction

In this section, we discuss the design of Lyapunov's control for the COVID-19 model with vaccine and treatment control [2], [26], [31]. The control design aims to overcome the nonlinearity and instability in the mathematical model of COVID-19 in the system (1). System (1) can be written in the following form:

$$\mathrm{x} = f(x, u, t), \tag{9}$$

where $\mathrm{x} = (S, E, I, R)$, $\mathrm{u} = (u_1, u_2)$. The system (1) is referred to as the actual system. Furthermore, the Lyapunov Quadratic Function (LQF) will be used to analyze the system (1) and develop appropriate control designs to stabilize and control the spread of COVID-19. First, a reference system (10) is established as:

$$\dot{x_d} = Fx_d, \begin{pmatrix} S \\ E \\ I \\ R \end{pmatrix} = \begin{pmatrix} -\mu & 0 & -\beta_1 & 0 \\ 0 & -(\alpha+\mu) & \beta_1 & 0 \\ 0 & \alpha & -(\varepsilon+\mu) & 0 \\ 0 & 0 & \varepsilon & -\mu \end{pmatrix} \begin{pmatrix} S \\ E \\ I \\ R \end{pmatrix}. \tag{10}$$

The parameter β_1 is the infection rate selected so that the reference model on the system (10) meets the disease-free condition. The magnitude of the error between the reference model (10) and the actual system (1) is defined as (11):

$$\begin{aligned} e &= x_d - x \\ \dot{e} &= \dot{x_d} - \dot{x} \end{aligned} \tag{11}$$

Substitute the system (1) and system (10) into (11) will obtained.

$$\begin{aligned} \dot{e} &= Fx_d - f(x, u, t) \\ \dot{e} &= Fx_d - Fx + Fx - f(x, u, t) \\ \dot{e} &= Fe + Fx - f(x, u, t) \end{aligned} \tag{12}$$

Lyapunov quadratic function (LQF) defined as (13):

$$V(e) = e^T P e, \tag{13}$$

where P is real symmetry and positive definite matrix.

Differentiate (13) over t will gives:

$$\begin{aligned} \dot{V}(e) &= \dot{e}^T P e + e^T P \dot{e} \\ \dot{V}(e) &= e^T (F^T P + PF) e + 2e^T P[Fx - f(x, z, u, t)] \\ \dot{V}(e) &= -e^T Q e + 2M \end{aligned} \tag{14}$$

where

$$F^T P + PF + Q = 0, \text{ and} \tag{15}$$

$$M = e^T P[Fx - f(x, u, t)]. \tag{16}$$

Then, substitute the system (1) and (10) into (16) will obtain:

$$\begin{aligned} M &= e^T P[Fx - f(x, u, t)] \\ &= (e_1 \quad e_2 \quad e_3 \quad e_4) \begin{pmatrix} p_{11} & p_{12} & p_{13} & p_{14} \\ p_{12} & p_{22} & p_{23} & p_{24} \\ p_{13} & p_{23} & p_{33} & p_{34} \\ p_{14} & p_{24} & p_{34} & p_{44} \end{pmatrix} \\ &\left[\begin{pmatrix} -\beta_1 I - \mu S \\ \beta_1 I - (\alpha+\mu)E \\ \alpha E - (\varepsilon+\mu)I \\ \varepsilon I - \mu R \end{pmatrix} - \begin{pmatrix} b + \phi R - (1-u_1 p)\beta SI - u_1 pS - \mu S \\ (1-u_1 p)\beta SI - (\alpha+\mu)E - u_1 pE \\ \alpha E - (1+u_2)\varepsilon I - \mu I \\ (1+u_2)\varepsilon I + u_1 pS + u_1 pE - (\phi+\mu)R \end{pmatrix} \right] \end{aligned}$$

$$= (r_1 \quad r_2 \quad r_3 \quad r_4)\begin{pmatrix} -\beta_1 I - b - \phi R + (1-u_1 p)\beta SI + u_1 pS \\ \beta_1 I - (1-u_1 p)\beta SI + u_1 pE \\ u_2 \varepsilon I \\ -u_2 \varepsilon I - u_1 pS - u_1 pE + \phi R \end{pmatrix}$$
$$= r_1(-\beta_1 I - b - \phi R + \beta SI) + r_2(\beta_1 I - \beta SI) + r_4 \phi R + u_1 p\big((r_2 - r_1)\beta SI + (r_1 - r_4)S + (r_2 - r_4)E\big) + u_2 \varepsilon I(r_3 - r_4), \quad (17)$$

where $r_1 = e_1 p_{11} + e_2 p_{12} + e_3 p_{13} + e_4 p_{14}$, $r_2 = e_1 p_{12} + e_2 p_{22} + e_3 p_{23} + e_4 p_{24}$, $r_3 = e_1 p_{13} + e_2 p_{23} + e_3 p_{33} + e_4 p_{34}$, $r_4 = e_1 p_{14} + e_2 p_{24} + e_3 p_{34} + e_4 p_{44}$,
Let

$$u_1 = \frac{-r_1(-\beta_1 I - b - \phi R + \beta SI) - c_1 S^2 - c_2 E^2 + c_3 S^2 sign(r_1) + c_4 E^2 sign(r_3)}{p\big((r_2 - r_1)\beta SI + (r_1 - r_4)S + (r_2 - r_4)E\big)}, \quad (18)$$

$$u_2 = \frac{-r_2(\beta_1 I - \beta SI) - r_4 \phi R - c_5 I^2 + c_6 I^2 sign(r_2)}{\varepsilon I(r_3 - r_4)}. \quad (19)$$

Substitute (18) and (19) into (17) then we obtained

$$M = -c_1 S^2 - c_2 E^2 + c_2 S^2 sign(r_1) + c_4 E^2 sign(r_3) - c_5 I^2 + c_6 I^2 sign(r_2). \quad (20)$$

Therefore, (14) become

$$\dot{V}(e) = -e^T Q e + 2(-c_1 S^2 - c_2 E^2 + c_3 S^2 sign(r_1) + c_4 E^2 sign(r_3) - c_5 I^2 + c_6 I^2 sign(r_2)). \quad (21)$$

Next, the matrix P will be solved from (15). In general, the parameter values in the controller design are determined by tuning. However, in this study, optimization was carried out using a genetic algorithm to obtain the parameter values c_i, $i = 1, \dots, 6$, of the control designs (18) and (19) that met $\dot{V}(e) < 0$ so that the system was stable.

3.4. Results of numerical simulation

In this section, a numerical simulation of the control design obtained from (20). The overview of the control strategy is given in Figure 1. Three control scenarios will be reviewed, namely control u_1 only, control u_2 only, and control u_1 & u_2 simultaneously. The initial value used in this simulation is $(S, E, I, R) = (0.980047, 8.6596 \times 10^{-4}, 0.001740, 0.017347)$ with a simulation time of 100 days. The parameter values of the COVID-19 mathematical model use the values in Table 1.

3.4.1. Scenario 1 (control u_1 only)

Simulations were carried out by applying only vaccination controls, namely $u_1 \neq 0$ and $u_2 = 0$. The value of the control design parameter estimates for scenario 1 is shown in Table 2. The graph of the control effort u_1 for implementing scenario 1 is given in Figure 3. The dynamics of each population based on the application of control u_1 is given in Figure 4. Based on Figure 3, the amount of control u_1 is given quite high at the beginning of the observation period then it decreases slowly until the end. Figure 4 shows that by giving control of vaccination to susceptible and exposed populations causes a decrease in both populations while increasing the immune population. Figure 4(a) shows that the number of susceptible humans decreased drastically and relatively quickly due to the implementation of vaccination control. The susceptible population will change phase to become an immune population, resulting in a drastic increase in the immune population, as seen in Figure 4(b). Figures 4(c) and 4(d) show that the exposed and infected individual populations have not been able to follow the reference curve well. However, in general, vaccination control reduced the exposed and infected population.

Table 2. Controller's parameter value of scenario 1, 2, and 3

Scenario 1		Scenario 2		Scenario 3	
Parameter	Value	Parameter	Value	Parameter	Value
c_1	0.89336	c_1	0.91366	c_1	0.91366
c_2	0.55222	c_2	0.29210	c_2	0.29210
c_3	0.89274	c_3	0.75015	c_3	0.75015
c_4	0.90952	c_4	0.26440	c_4	0.26440
c_5	0.96515	c_5	0.96002	c_5	0.96002
c_6	0.31483	c_6	0.93945	c_6	0.93945

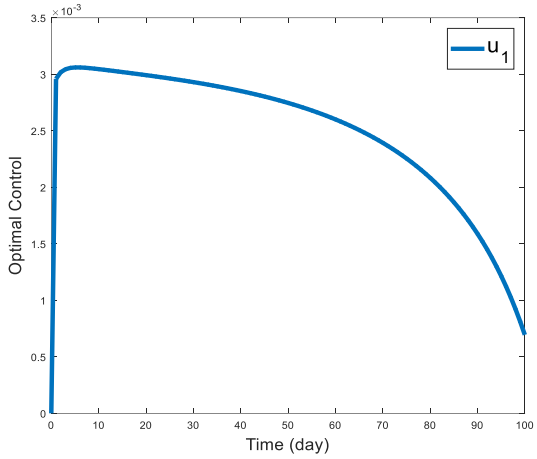

Figure 3. Optimal control u_1 of scenario 1

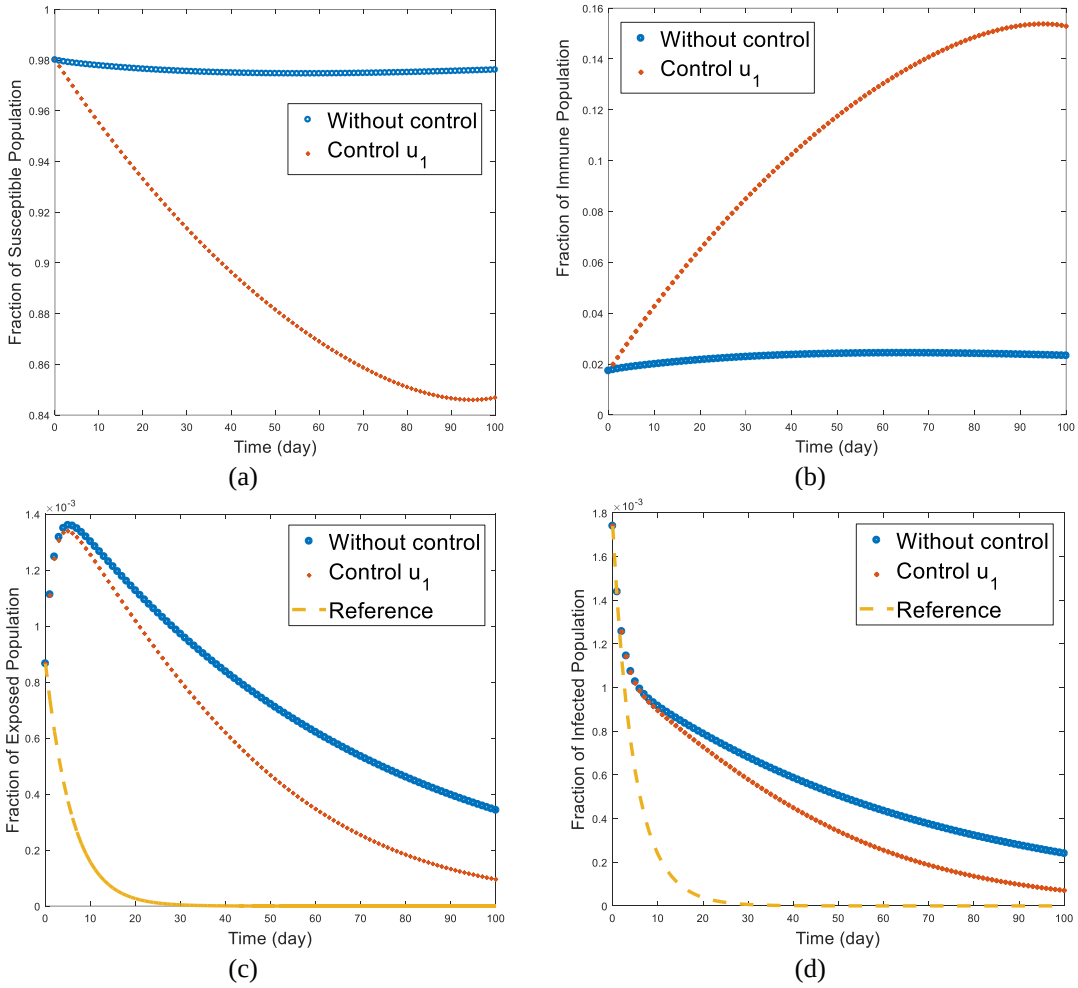

Figure 4. The dynamics of (a) S, (b) E, (c) I, and (d) R for scenario 1

3.4.2. Scenario 2 (control u_2 only)

The simulation was carried out by applying only treatment controls, namely $u_2 \neq 0$ and $u_1 = 0$. The value of the control design parameter estimation results for scenario 2 is shown in Table 2. The graph of the optimal control u_2 for implementing scenario 2 is given in Figure 5. The dynamics of each population based on the application of control u_2 is given in Figure 6. Based on Figure 5, the amount of control effort is given

with a high portion at the beginning of the observation period, and then it decreases slowly until it reaches zero on the 65th day and ends. Figure 6 shows that administration of control treatment succeeded in significantly reducing the number of exposed and infected individual populations. While Figure 6(a) shows that the susceptible population experienced an increase, Figure 6(b) shows a significant decrease in the exposed individual. Figure 6(c) shows that the curve of infected individuals is able to follow the reference curve quite well. In addition, in Figure 6(d), the population of immune individuals decreased. This happens because of the assumption that immunity is temporary so that immune individuals return to being susceptible individuals.

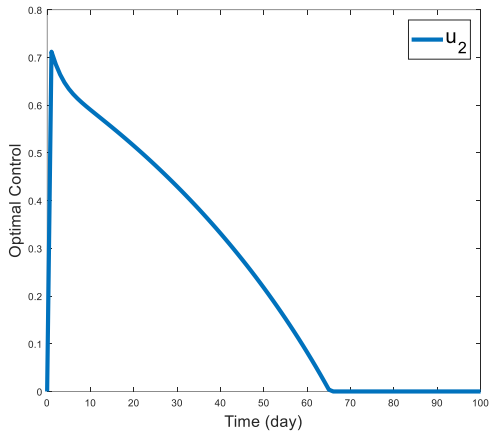

Figure 5. Optimal control value u_2 of scenario 2

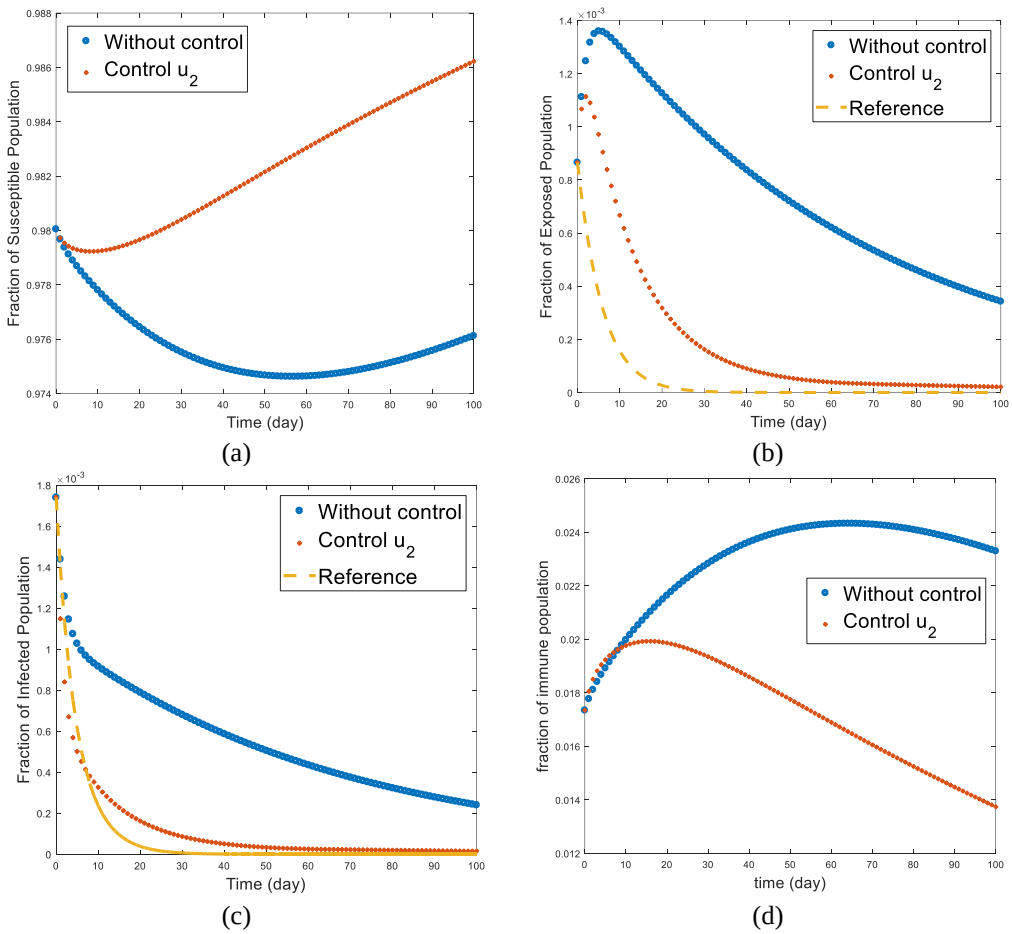

Figure 6. The dynamics of (a) S, (b) E, (c) I, and (d) R for scenario 2

3.4.3. Scenario 3 (control u_1 and u_2 simultaneously)

Simulations were carried out by applying only treatment controls, namely $u_2 \neq 0$ and $u_1 \neq 0$. The estimated control design parameter values for scenario 3 are shown in Table 2. The graphs of the control effort u_1 and u_2 for the implementation of scenario 3 are given in Figure 7. The dynamics of each population are given in Figure 8. Based on Figure 7, the amount of control effort u_1 is given is relatively low during the observation time. The amount of control effort u_1 is given is quite high at the beginning of the observation period and then decreases slowly until the end of the observation period. While the amount of control effort u_2 is given with a high portion at the beginning of the observation period. Then it decreased slowly until it reached zero on the 65th day until the end of the observation time.

Figure 8 shows the dynamics of each population based on the application of control scenario 3. The administration of control of vaccination and treatment simultaneously succeeded in reducing the number of exposed and infected individual populations significantly. In Figure 8(a) the population of susceptible individuals has significantly decreased. In Figure 8(b), the population of exposed individuals decreases significantly following the reference model. In addition, Figure 8(c) shows that the curve of infected individuals is able to follow the reference curve quite well, while in Figure 8(d) the immune population has increased. This happened because of the implementation of vaccination control in susceptible individuals.

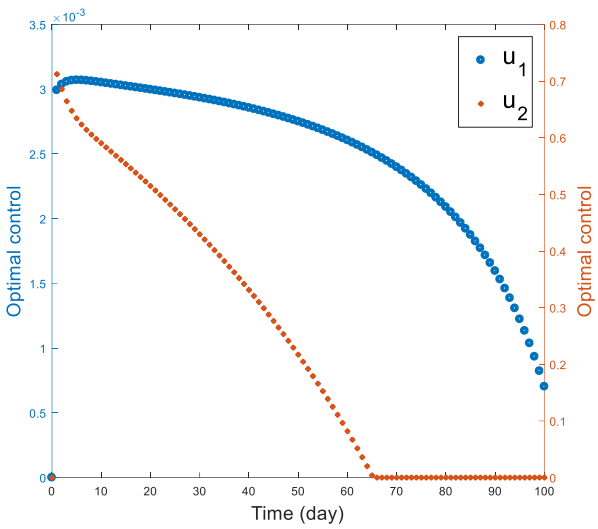

Figure 7. Optimal control value of u_1 and u_2 for scenario 3

Table 3 compares the number of individuals exposed and infected at the end of the observation period for each scenario. Table 3 shows that implementing the three scenarios may decrease the exposed and infected populations by the end of the observation period (day 100). The application of scenario 1 (vaccination) was able to lower the number of people exposed to the disease by 72.21% and the number of people who were infected by 70.53% over the observation period. By implementing scenario 2 (vaccination), it was possible to lower the number of people exposed to human disease by 93.80% and the number of people infected by 93.81%. The most significant reduction was achieved by implementing scenario 3 (vaccination and concurrent treatment), which led to a 98.29% decrease in the population of exposed humans and a 98.18% decrease in infected humans.

Table 3. The comparison of exposed & infected population in the end of simulation (day-100th)

Condition	Exposed Population (E)	Infected Population (I)	The reduction percentage of exposed population	The reduction percentage of infected population
Without control	3854 people	2698 people	-	-
Control u_1	1071 people	795 people	72.21%	70.53%
Control u_2	239 people	167 people	93.80%	93.81%
Control u_1 & u_2 simultaneously	66 people	49 people	98.29%	98.18%

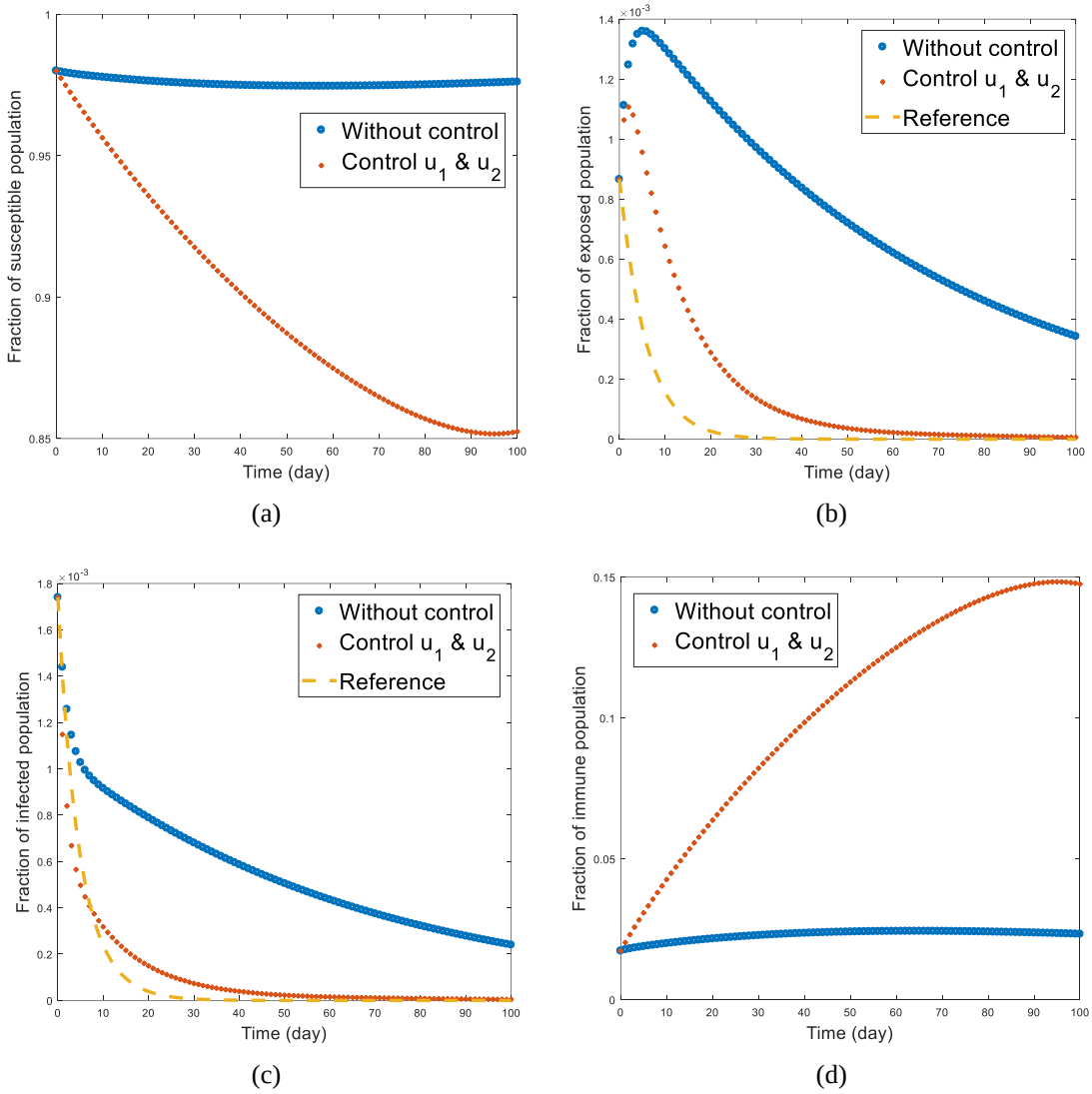

Figure 8. The dynamics of (a) S, (b) E, (c) I, and (d) R for scenario 3

4. CONCLUSION

A mathematical model of the spread of COVID-19 with control variables of vaccination and treatment has been studied. Parameter values in the model have been obtained using parameter estimation with genetic algorithms. An analysis of the stability of the equilibrium points and the basic reproduction number of the COVID-19 model has been carried out. Then, a control design based on the Lyapunov function was developed to stabilize the system and reduce the population of exposed and infected individuals. Furthermore, numerical simulations were carried out with three control scenarios, namely control vaccination only, control treatment only, and both controls simultaneously. The controller parameter values have been estimated using a genetic algorithm. Based on the results of numerical simulations, scenario 3 (vaccination and concurrent treatment) gave the most significant decrease, namely the average decrease in the exposed human population by 98.29% and the infected human population by 98.18%.

REFERENCES

[1] Y. Longueira, M. L. Polo, G. Turk, and N. Laufer, "Dynamics of SARS-CoV-2-specific antibodies among COVID19 biobank donors in Argentina," *Heliyon*, vol. 7, no. 10, Oct. 2021, doi: 10.1016/j.heliyon.2021.e08140.

[2] D. Vlachakis *et al.*, "Molecular mechanisms of the novel coronavirus SARS-CoV-2 and potential anti-COVID19 pharmacological targets since the outbreak of the pandemic," *Food and Chemical Toxicology*, vol. 146, no. August, p. 111805, 2020, doi: 10.1016/j.fct.2020.111805.

[3] S. R. Neely and F. Hao, "Breakthrough COVID-19 infections and perceived vaccine effectiveness," *Vaccine*, vol. 41, no. 52, pp. 7689–7694, Dec. 2023, doi: 10.1016/j.vaccine.2023.11.032.

[4] F. Kakuya *et al.*, "Epidemiology of endemic human coronavirus infection during the COVID-19 pandemic," *Journal of Infection and Chemotherapy*, vol. 30, no. 5, pp. 400–405, May 2024, doi: 10.1016/j.jiac.2023.11.012.

[5] Y. Li, J. Lan, and G. Wong, "Advances in treatment strategies for COVID-19: insights from other coronavirus diseases and prospects," *Biosafety and Health*, vol. 5, no. 5, pp. 272–279, Oct. 2023, doi: 10.1016/j.bsheal.2023.08.003.

[6] M. Haque, F. Al Basir, E. Venturino, A. Saeed, and S. R. Smith, "Mathematical modelling of clonorchiasis with human treatment and fish vaccination versus snail control," *Chaos, Solitons & Fractals*, vol. 167, Feb. 2023, doi: 10.1016/j.chaos.2022.113048.

[7] J. Zhang, L. Liu, Y. Li, and Y. Wang, "An optimal control problem for dengue transmission model with Wolbachia and vaccination," *Communications in Nonlinear Science and Numerical Simulation*, vol. 116, Jan. 2023, doi: 10.1016/j.cnsns.2022.106856.

[8] R. G. S. de Araújo, D. C. P. Jorge, R. C. Dorn, G. Cruz-Pacheco, M. L. M. Esteva, and S. T. R. Pinho, "Applying a multi-strain dengue model to epidemics data," *Mathematical Biosciences*, vol. 360, Jun. 2023, doi: 10.1016/j.mbs.2023.109013.

[9] S. Paul, A. Mahata, U. Ghosh, and B. Roy, "Study of SEIR epidemic model and scenario analysis of COVID-19 pandemic," *Ecological Genetics and Genomics*, vol. 19, May 2021, doi: 10.1016/j.egg.2021.100087.

[10] S. Annas, M. Isbar Pratama, M. Rifandi, W. Sanusi, and S. Side, "Stability analysis and numerical simulation of SEIR model for pandemic COVID-19 spread in Indonesia," *Chaos, Solitons and Fractals*, vol. 139, p. 110072, 2020, doi: 10.1016/j.chaos.2020.110072.

[11] Q. Sun, T. Miyoshi, and S. Richard, "Analysis of COVID-19 in Japan with extended SEIR model and ensemble Kalman filter," *Journal of Computational and Applied Mathematics*, vol. 419, Feb. 2023, doi: 10.1016/j.cam.2022.114772.

[12] C. Xu, Y. Yu, G. Ren, Y. Sun, and X. Si, "Stability analysis and optimal control of a fractional-order generalized SEIR model for the COVID-19 pandemic," *Applied Mathematics and Computation*, vol. 457, Nov. 2023, doi: 10.1016/j.amc.2023.128210.

[13] A. ElHassan, Y. AbuHour, and A. Ahmad, "An optimal control model for Covid-19 spread with impacts of vaccination and facemask," *Heliyon*, vol. 9, no. 9, Sep. 2023, doi: 10.1016/j.heliyon.2023.e19848.

[14] Fatmawati, C. W. Chukwu, R. T. Alqahtani, C. Alfiniyah, F. F. Herdicho, and Tasmi, "A Pontryagin's maximum principle and optimal control model with cost-effectiveness analysis of the COVID-19 epidemic," *Decision Analytics Journal*, vol. 8, Sep. 2023, doi: 10.1016/j.dajour.2023.100273.

[15] A. Venkatesh and M. Ankamma Rao, "Mathematical model for COVID-19 pandemic with implementation of intervention strategies and cost-effectiveness analysis," *Results in Control and Optimization*, vol. 14, Mar. 2024, doi: 10.1016/j.rico.2023.100345.

[16] A. Kouidere, O. Balatif, and M. Rachik, "Cost-effectiveness of a mathematical modeling with optimal control approach of spread of COVID-19 pandemic: a case study in Peru," *Chaos, Solitons & Fractals: X*, vol. 10, Jun. 2023, doi: 10.1016/j.csfx.2022.100090.

[17] P. Yarsky, "Using a genetic algorithm to fit parameters of a COVID-19 SEIR model for US states," *Mathematics and Computers in Simulation*, vol. 185, pp. 687–695, Jul. 2021, doi: 10.1016/j.matcom.2021.01.022.

[18] Y. Zelenkov and I. Reshettsov, "Analysis of the COVID-19 pandemic using a compartmental model with time-varying parameters fitted by a genetic algorithm," *Expert Systems with Applications*, vol. 224, Aug. 2023, doi: 10.1016/j.eswa.2023.120034.

[19] A. Kara, "Multi-step influenza outbreak forecasting using deep LSTM network and genetic algorithm," *Expert Systems with Applications*, vol. 180, Oct. 2021, doi: 10.1016/j.eswa.2021.115153.

[20] C. Kuptametee, Z.-H. Michalopoulou, and N. Aunsri, "A review of efficient applications of genetic algorithms to improve particle filtering optimization problems," *Measurement*, vol. 224, Jan. 2024, doi: 10.1016/j.measurement.2023.113952.

[21] M. I. Azeez and K. R. Atia, "Modeling of PID controlled 3DOF robotic manipulator using Lyapunov function for enhancing trajectory tracking and robustness exploiting Golden Jackal algorithm," *ISA Transactions*, vol. 145, pp. 190–204, Feb. 2024, doi: 10.1016/j.isatra.2023.11.033.

[22] V. C. Nguyen, H. L. Thi, and T. L. Nguyen, "A Lyapunov-based model predictive control strategy with a disturbances compensation mechanism for dual-arm manipulators," *European Journal of Control*, vol. 75, Jan. 2024, doi: 10.1016/j.ejcon.2023.100913.

[23] C. Cavallaro, V. Cutello, M. Pavone, and F. Zito, "Machine learning and genetic algorithms: a case study on image reconstruction," *Knowledge-Based Systems*, vol. 284, Jan. 2024, doi: 10.1016/j.knosys.2023.111194.

[24] M. Neghină, A.-I. Dicoiu, R. Chiş, and A. Florea, "A competitive new multi-objective optimization genetic algorithm based on apparent front ranking," *Engineering Applications of Artificial Intelligence*, vol. 132, Jun. 2024, doi: 10.1016/j.engappai.2024.107870.

[25] D. Cohen *et al.*, "Predictors of reinfection with pre-Omicron and Omicron variants of concern among individuals who recovered from COVID-19 in the first year of the pandemic," *International Journal of Infectious Diseases*, vol. 132, pp. 72–79, Jul. 2023, doi: 10.1016/j.ijid.2023.04.395.

[26] A. Sa'adah, R. Saragih, and D. Handayani, "Application of Lyapunov control for analysis spread of COVID-19 in Indonesia," *9th 2023 International Conference on Control, Decision and Information Technologies, CoDIT 2023*, no. 10, pp. 1238–1243, 2023, doi: 10.1109/CoDIT58514.2023.10284103.

[27] K. G. Mekonen, F. M. Aragaw, and K. T. Aknda, "Optimal control analysis on the impact of non-pharmaceutical interventions and vaccination on the dynamics of COVID-19," *Results in Control and Optimization*, vol. 13, 2023, doi: 10.1016/j.rico.2023.100319.

[28] M. Kamrujjaman, P. Saha, M. S. Islam, and U. Ghosh, "Dynamics of SEIR model: a case study of COVID-19 in Italy," *Results in Control and Optimization*, vol. 7, 2022, doi: 10.1016/j.rico.2022.100119.

[29] N. K. Goswami, S. Olaniyi, S. F. Abimbade, and F. M. Chuma, "A mathematical model for investigating the effect of media awareness programs on the spread of COVID-19 with optimal control," *Healthcare Analytics*, vol. 5, 2024, doi: 10.1016/j.health.2024.100300.

[30] P. Wintachai and K. Prathom, "Stability analysis of SEIR model related to efficiency of vaccines for COVID-19 situation," *Heliyon*, vol. 7, no. 4, 2021, doi: 10.1016/j.heliyon.2021.e06812.

[31] H. I. Ali and M. A. Hadi, "Optimal nonlinear controller design for different classes of nonlinear systems using black hole optimization method," *Arabian Journal for Science and Engineering*, vol. 45, no. 8, pp. 7033–7053, 2020, doi: 10.1007/s13369-020-04650-z.

BIOGRAPHIES OF AUTHORS

Aminatus Sa'adah received the B.Sc. degree in mathematics from Universitas Airlangga, Indonesia in 2018 and the M.Sc. degrees in mathematics from Institut Teknologi Bandung, Indonesia, in 2022. Currently, she is a lecturer at the Department of Informatics Engineering, Institut Teknologi Telkom Purwokerto (now Telkom University Purwokerto) Indonesia. Her research interests include disease mathematical modeling, optimization, control theory, particle swarm optimization, and deep learning. She can be contacted at email: aminatussaadah.math@gmail.com or aminatus@ittelkom-pwt.ac.id.

Roberd Saragih received the B.Sc. degree in mathematics from Institut Teknologi Bandung, Indonesia, in 1986, the M.Sc. degrees in instrumental and control from Institut Teknologi Bandung, Indonesia, in 1993, and Ph.D. degrees in mechanical engineering from Keio University, Japan, in 1998. Currently, he is a mathematics professor at Institut Teknologi Bandung specialized in control and optimization. His research interests include optimal control theory, applied mathematics, optimization, mechanical control and system. He can be contacted at email: roberd@itb.ac.id or roberdsaragih58@gmail.com.

Dewi Handayani received the B.Sc. degree, M.Sc. degrees, and Ph.D. degrees in mathematics from Institut Teknologi Bandung in 2011, 2012, and 2017 respectively. Currently, he is a mathematics lecturer at Institut Teknologi Bandung specialized in control and optimization. His research interests include disease modeling, optimal control theory, applied mathematics, optimization. She can be contacted at email: dhandayanimtk@itb.ac.id or dewihandayansutisna@gmail.com.